TRENDS IN SCIENCES 2025; 22(12): 11044
https://doi.org/10.48048/tis.2025.11044
RESEARCH ARTICLE

Thermo-Physical Enhancement of Paraffin Based Phase Change Materials with Iron Sand (Fe_3O_4) for Application in Building Thermal Management

Widya Sonita Gultom[1], Timbangen Sembiring[1,*], Anggito Pringgo Tetuko[2], Muhammad Fauzi[1,2,3], Amdy Fachredzy[2,3], Eko Arief Setiadi[2], Nining Sumawati Asri[2], Ayu Yuswita Sari[2], Martha Rianna[1], Erna Frida[1] and Achmad Maulana Soehada Sebayang[1]

[1]Department of Physics, Faculty of Mathematics and Natural Sciences, Universitas Sumatera Utara, Medan 20155, Indonesia
[2]Research Center for Advanced Materials, National Research and Innovation Agency (BRIN), Tangerang Selatan 15314, Indonesia
[3]Department of Physics, Faculty of Mathematics and Natural Sciences, Universitas Indonesia, Depok 16424, Indonesia

([*]Corresponding author's e-mail: timbangen@usu.ac.id)

Received: 23 June 2025, Revised: 9 July 2025, Accepted: 16 July 2025, Published: 10 September 2025

Abstract

This study investigates the encapsulation and thermal performance of paraffin-based phase change materials (PCM) enhanced with magnetite (Fe_3O_4) nanoparticles for building energy storage applications. The PCM composite was encapsulated within 4 copper tubes (1.27 cm in diameter and 5 cm in length), which were embedded into concrete specimens measuring 5×5×5 cm^3. The concrete samples were cured at room temperature for 28 days. The paraffin-magnetite mixture was homogenized via ultrasonic sonication at 80 °C for 15 min at 37 kHz to ensure uniform nanoparticle dispersion and minimize agglomeration. X-ray diffraction analysis confirmed the crystalline nature of magnetite and the semi-crystalline monoclinic structure of paraffin. The addition of magnetite enhanced the magnetic properties of the composite, with saturation magnetization reaching 30 emu/g at 50 %vol Fe_3O_4. Differential Scanning Calorimetry revealed a reduction in latent heat to 17.13 J/g due to the incorporation of magnetite, while the thermal conductivity increased significantly to 0.54 W/m·K. These results indicate that although latent heat decreases, the improved thermal conductivity contributes to enhanced heat transfer during the phase transition. Overall, the integration of Fe_3O_4 nanoparticles into paraffin-based PCM demonstrates promising potential for improving the thermal energy storage performance in building applications.

Keywords: Phase change materials, Paraffin, Macro-encapsulation, Magnetite particles, Management thermal, Thermal storage

Introduction

The building construction sector accounts for approximately 40% of the total energy consumption worldwide. This share will increase as the energy consumption for space heating and cooling increases to 12% and 37%, respectively, in 2050. It has been reported that building construction and activities provided 36% of the global energy used in buildings and 39% of energy-related carbon dioxide emissions in 2018 [1,2]. Therefore, measures should be taken to limit this consumption by introducing various renewable energy technologies and systems [3,4]. Thermal Energy Storage (TES) is one of the most important technologies for renewable energy storage that can manage heat, e.g., latent heat, sensible heat, and chemical heat [5]. TES systems can store excess heat energy using appropriate media; therefore, the stored energy can be withdrawn and reused when required in certain processes. Among these, latent heat storage using Phase Change Materials

(PCM) is widely recognized for its high energy density and narrow operating temperature range, making it ideal for passive thermal regulation [6,7].

Thermal bonding agents, such as Phase Change Materials (PCM), can be utilized to improve thermal performance with less effect on existing structural properties. PCM are capable of changing phase at a given temperature, enabling latent heat absorption and release. This allows PCM to shift peak temperature loads and maintain indoor thermal comfort more effectively [8-10]. Many materials combining organic and inorganic substances have been used as PCM. The selection of PCM materials is typically based on thermal reliability, phase change temperature, chemical stability, and cost. Inorganic PCM have high latent heat capacity but are often corrosive. Organic PCM - such as paraffin - are non-toxic, chemically stable, and exhibit relatively high latent heat [11,12]. Paraffin, a saturated alkane with the empirical formula C_nH_{2n+2}, is widely used in thermal energy storage applications. It offers good chemical compatibility and a broad melting point range. However, its low thermal conductivity (< 0.3 W/m·K) is a limiting factor, particularly in applications requiring rapid heat exchange [13]. To overcome this, many researchers have explored the addition of thermally conductive materials into PCM.

A considerable number of studies have reported thermal enhancement achieved by dispersing metal nanoparticles in PCM, including Fe_3O_4 [14], TiO_2 [15], SiO_2 [16], Al_2O_3 and MgO [17]. Carbon-based materials such as carbon nanotubes (CNTs) [18], graphene [19], and carbon fibers [20] have also been used to increase conductivity. In Singh *et al.* [17], various nanomaterials (SiO_2, Al_2O_3 and MgO) at 0.1 - 0.5 vol% were added to paraffin, yielding significant increases in thermal conductivity (10.71% - 29.32%) and viscosity (up to 90%). In another study, Prabhu *et al.* [21] added 7.5 and 10 wt% of Al_2O_3 nanoparticles to paraffin, producing latent heat values of 203.89 and 187.44 kJ/kg and enhancing thermal conductivity by 42% and 57% compared to pure paraffin. However, high nanoparticle loading often compromises energy storage capacity due to volume displacement. He *et al.* [22]; He *et al.* [23] investigated the thermal and magnetic properties of Fe_3O_4-paraffin composites at 1 - 3 wt%. Thermal conductivity improved from 0.251 to 0.331 W/m·K, but latent heat declined with increasing Fe_3O_4 content. These results confirm that increasing filler content improves thermal conductivity but may reduce heat storage performance, emphasizing the need to optimize composition for target applications. Furthermore, carbon-based materials can be utilized to improve the thermal conductivity of PCM. Fikri *et al.* [18] investigated multi-walled carbon nanotubes (MWCNTs) as thermal enhancers and reported a 150.7% increase in thermal conductivity with the addition of 1 wt% MWCNTs - reaching 0.597 W/m·K compared to 0.238 W/m·K for pure A70 paraffin. Hu *et al.* [24] explored hybrid PCM composites using CNTs (2 wt%) and styrene-butadiene-styrene (SBS) at 18 - 8 wt%, processed at 180 °C. Although melting enthalpy decreased from 200.01 J/g (pure paraffin) to 142.28 - 157.70 J/g, the materials retained good morphological and mechanical integrity making them promising for TES. Sharshir *et al.* [25] examined paraffin doped with CuO, Co_3O_4, and CuO@Co_3O_4 (each 3 wt%). The synthesis involved magnetically assisted stirring at 60 °C and sonication. Morphological and EDX analyses confirmed uniform dispersion of the nanoparticles. Despite some reduction in melting enthalpy (11% - 20%), the nanocomposites exhibited improved thermal responsiveness and stability.

Previous studies have shown that conductive nanoparticles not only improve thermal conductivity but can also enhance thermal storage capacity [26,27]. However, most of these enhancements are studied at the material level, and their performance in real structural systems like concrete remains less explored. The integration of PCM into cementitious systems is gaining interest due to their potential in passive thermal regulation. Concrete, as a widely used building material, is an ideal carrier for PCM because of its formability, availability, and mechanical properties. Additional benefits include dampening thermal fluctuations and reducing freeze–thaw-related damage in cold climates [28]. PCM can be incorporated into concrete either directly or indirectly. In this study, an indirect approach is adopted [29], using microencapsulation.

This method places the PCM inside sealed containers (e.g., tubes or spheres) embedded into the concrete, preventing leakage and minimizing interference with the concrete's structural function. It also improves both thermal and mechanical properties of the PCM-concrete composite [28]. Al-Yasiri *et al.*

[30] investigated aluminum macroencapsulation in concrete and reported improved thermal behavior and extended retention times, especially under high outdoor temperatures. Thermal transfer rates increased with encapsulation surface area. In addition, Tetuko *et al.* [13] enhanced paraffin with 50% magnetite and showed that thermal conductivity rose from 0.32 to 0.53 W/m·K. The encapsulated system effectively stored and released heat during cyclic operation.

Comparatively, microencapsulation approaches such as those studied by Alsaadawi *et al.* [31] showed reduced peak temperatures (6.75 - 9.25 °C) when 1% - 10% microencapsulated PCM was added. However, compressive strength decreased, requiring higher target design strengths (~40 MPa). Despite some paraffin leakage upon shell breakage, PCM helped refine the interface between aggregate and cement paste. Ying *et al.* [32] implemented graded PCM aggregates to enable multi-stage latent heat release between 5 and −15 °C, mitigating frost heave in cold regions. Yet, as PCM content increased, compressive strength showed a declining trend-reinforcing the performance trade-off in structural applications. Although many advances have been made, few studies focus on natural fillers such as Fe_3O_4 from iron sand, or on scalable macroencapsulation systems embedded directly in concrete. This study aims to address both gaps.

In this research, paraffin is enhanced with natural Fe_3O_4 particles sourced from West Java, Indonesia. The composite is macroencapsulated in 4 copper tubes and embedded into concrete blocks. Copper was selected for its high thermal conductivity and compatibility with cementitious materials. The Fe_3O_4 content is varied at 20, 30, 40 and 50 vol% to evaluate its effect on thermal and magnetic behavior. The novelty of this study lies in 3 main aspects: (i) the use of natural, low-cost Fe_3O_4 as a thermally and magnetically active additive, (ii) the design of a practical copper-tube macroencapsulation system embedded in concrete, and (iii) the focus on real-world structural integration for building thermal energy management. The objective is to evaluate the thermophysical, magnetic, and structural performance of the PCM-concrete system and determine its feasibility as a passive energy storage solution.

Materials and methods

Materials

Paraffin with a nominal melting point of 50 - 60 °C was used as the organic phase change material (PCM), which was acquired from a local supplier. An improvement in thermal conductivity was achieved by the addition of magnetite particles. The magnetite used in this research was obtained from the West Java region and mixed to form a paraffin-Fe_3O_4 composite phase change material (PCM). The physical and thermal properties of paraffin and Fe_3O_4 are summarized in **Table 1** [33]. In addition, concrete was used to install the copper tube and encapsulate the PCM. The raw material of the concrete comprised cement, river sand, water and aggregates and its properties are given in **Table 2** [34].

Table 1 Properties of paraffin and Fe_3O_4.

Specification (unit)	Paraffin	Magnetite-Fe_3O_4
Melting point (°C)	50 - 60	1,870
Laten heat (kJ/kg)	142	-
Thermal conductivity (W/m·K)	0.23	9.7
Density (kg/m^3)	760	7874

Table 2 Properties of aggregates.

Specification (unit)	Value
Maximum particle size (mm)	50
Unit weight (kg/m^3)	732
Apparent porosity (%)	18.1
Percent absorption (%)	17.5

Preparation of PCM

The preparation process of the PCM is shown in **Figure 1**. In this research, sonication heating was chosen because to its uniformity and rapid heating. The technique involves melting, stirring, sonication and solidification. Paraffin was first melted at 50 °C and Fe_3O_4 was then added to the melting paraffin. Fe_3O_4 was added according to the compositions listed in **Table 3**. During sonication, the suspension was stirred in an ultrasonic bath for 15 min at 80 °C, and ultrasonic frequency of 37 kHz was applied to achieve uniform dispersion and to avoid precipitation of nanoparticles. In the solidification step, the suspension was poured into a mold.

Table 3 Compositions of PCM samples.

Sample	Paraffin (%vol)	Magnetite-Fe_3O_4 (%vol)
PCM-A0	100	0
PCM-A1	80	20
PCM-A2	70	30
PCM-A3	60	40
PCM-A4	50	50

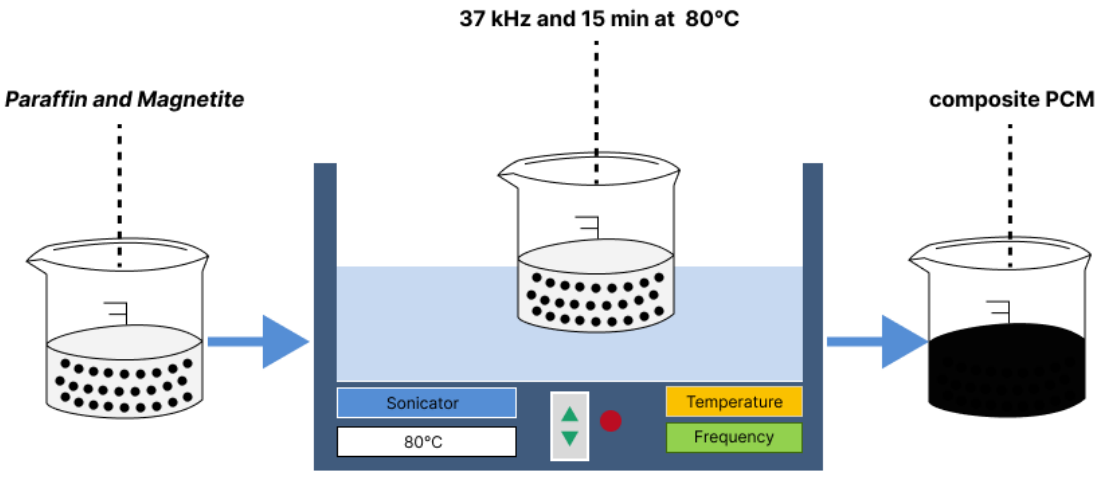

Figure 1 Preparation of PCM composite with ultrasonic bath technique.

Preparation of concrete samples

The concrete was constructed with dimensions of 5×5×5 cm^3. The concrete mix proportion was set to 0.7:2:1.5:1 (water: aggregates: river sand: cement). The concrete specimens were stored at room temperature for 28 days for the curing process. Four copper tubes with a diameter of 1.25 cm and length of 5 cm were used as the encapsulation media.

Characterizations

The crystalline paraffin and Fe_3O_4 phases of the PCM composite were determined using XRD (D/teX ultra250). The chemical structure of the PCM was analyzed using fourier transform infrared spectroscopy (FTIR; Thermoscientific Nicolet iS 10) in the range of 4,000 - 400 cm^{-1}. The morphology and microstructure of the shape-stabilized PCM were investigated using Scanning Electron Microscopy-Energy Dispersive X-Ray (SEM-EDX; SEM Hitachi, SU3500). The thermal stability of the shape-stabilized PCM was evaluated using a differential scanning calorimeter (DSC 8000, Perkin Elmer) to determine the latent heat and phase change temperature, which was carried out in a N_2 atmosphere from 30 to 150 °C at a heating/cooling rate of 10 °C min^{-1}. The thermal conductivities of the PCM were measured using a QTM-500-thin film instrument.

Experimental set-up

In this study, concrete was installed with 4 copper tubes as PCM encapsulation media. Several thermocouples connected to a data logger were installed in the PCM encapsulated concrete to monitor temperature distribution. A heater at a constant temperature of 80 °C was applied to the PCM encapsulated concrete as the heat source. Rock wool was utilized as an insulation material to minimize heat loss. The experimental setup is illustrated in **Figure 2**. All prepared PCM specimens were poured into a copper tube inside the concrete (5×5×5 cm^3). The samples consisted of 4 PCM specimens and were provided with an accurate calibrated measuring device to evaluate and compare their thermal performance. These devices use K-type thermocouples connected to an Arduino-based digital readout monitor. Temperature distribution measurements were conducted for 24 h per day. The temperature distribution experiment was conducted to test the thermal performance of PCM encapsulated in a concrete. The samples consisted of all PCM encapsulated concrete samples with different magnetite compositions.

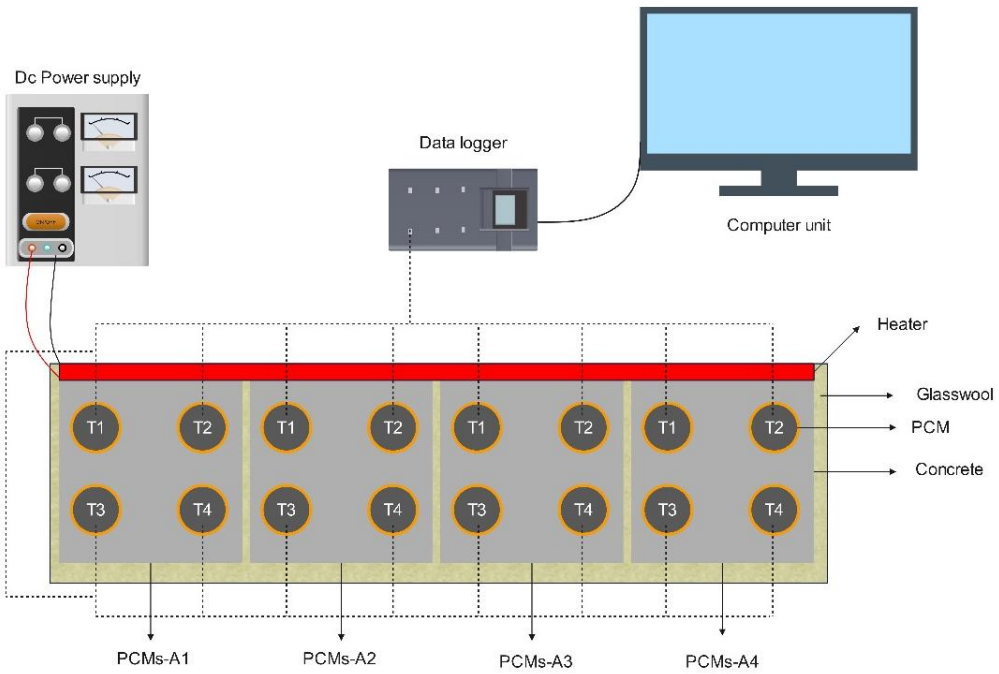

Figure 2 Temperature distribution experimental set-up of PCM encapsulated concrete.

Results and discussion

Sturctural characterization of paraffin and Fe_3O_4

The analysis of the XRD spectra provided important information on the structural properties, that is, the phase and crystallite size (D) [35]. The X-ray diffraction (XRD) patterns of paraffin and Fe_3O_4 are shown in **Figure 3**. The XRD pattern data of paraffin are reported at 2 diffraction peaks: 21.46° and 23.84° which indicate diffraction from the (110) and (200) crystal planes, respectively. Paraffin also has a monoclinic crystalline phase based on the standard data of COD-96-434-3587. Although paraffin has monoclinic crystal characteristics at room temperature, an increase in paraffin temperature causes the β phase in paraffin to gradually change into the α phase and thus the crystal structure of paraffin becomes hexagonal or orthorhombic [36,37]. The XRD spectra of Fe_3O_4 showed diffraction peaks at 30.16°, 35.49°, 43.03°, 53.35°, 56.96°, 62.46° and 73.93° with phase crystallites of (220) (311) (400) (422) (511) (440) and (642) for the cubic phase structure, which were confirmed using COD-96-151-3305 standard data [35]. The general method for determining the crystallite size from the XRD spectra is the Scherrer method [35], as shown in Eq. (1). Where D is the crystallite size, k is a geometric factor (0.9), λ is the wavelength of a copper target of X-ray (λ = 1.79), β is the full width at half maximum (FWHM) of the diffraction peak and θ is the diffraction angle [35,38].

The presence of sharp and well-defined peaks indicates a highly ordered lattice structure. While detailed calculations of lattice constants and full width at half maximum (FWHM) are not included in this study, they represent important parameters for future work to assess the degree of crystallinity and potential lattice strain more precisely.

$$\mathbf{D} = \frac{\mathbf{k\lambda}}{\boldsymbol{\beta}\ \mathbf{Cos}\ \boldsymbol{\theta}} \quad (1)$$

Based on the calculation, it was determined that the paraffin diameter was 3.93 nm while the Fe_3O_4 crystal size was 1.95 nm. However, due to the limitations of XRD in detecting low-angle grain boundaries or dislocation defects, further analysis using high-resolution TEM is recommended to investigate possible lattice imperfections and interfacial dislocations, which may play a role in phonon scattering and thermal conductivity behavior.

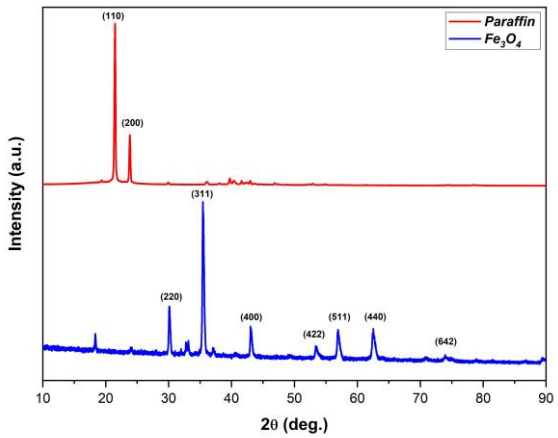

Figure 3 XRD patterns of paraffin and Fe_3O_4.

Chemical stability analysis of PCM

Infrared spectrograms of the synthesized specimens were measured using a Thermoscientific Nicolet iS-10 instrument with has a scanning range of (4,000 - 400 cm^{-1}). **Figure 4** shows the FTIR spectrum region of the PCM-A1 sample at 565.58 to 2,956.96 cm^{-1} and PCM-A4 sample at 570.48 to 3,444.50 cm^{-1}. The spectrum of Fe_3O_4 occurs at wave numbers 570.48 and 565.58 cm^{-1}, which is characteristic of magnetite (Fe_3O_4) where the group formed is Fe-O [39]. While at a wave number of 719.40 and 719.47 cm^{-1} are C-H functional groups, and 729 cm^{-1} is CH_2 groups. At peak of 1,377.48 and 1,377.40 cm^{-1} suggested the functional groups of CH_2 and O-H bonds [40]. The peak at 1,472

cm^{-1} indicates a CH_2 rocking vibration [41]. At wave numbers of 2,848 and 2,917 cm^{-1}, CH_2 represents an asymmetrical stretching vibration [42]. The peak at 2,956 cm^{-1} represents the O-H groups [43]. The comparison of FTIR the PCM-A1 and PCM-A4 samples showed no significant difference. This indicates that only physical mixing between paraffin and Fe_3O_4 occurred and did not damage the crystal structures of each other after the melting process. Thus, no new functional groups were formed in the PCM composites.

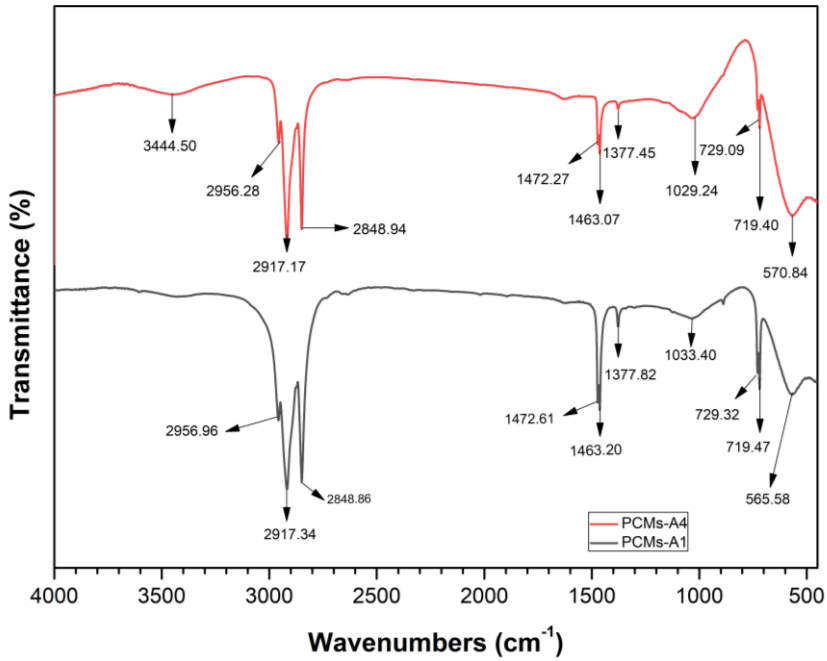

Figure 4 The results of FTIR spectra for PCM-A1 and PCM-A4 samples.

Morphology analysis of PCM

To determine the morphological structure of the PCM samples and the elemental content of the PCM, Scanning Electron Microscopy-Energy Dispersive X-Ray (SEM-EDX) was used. SEM-EDX characterization was carried out at a magnification of 5k, samples were characterized as PCM-A1 and PCM-A4. The SEM-EDX morphology results at 5k magnification are shown in **Figure 5**. The magnetite particles had a suitable distribution range and were spherical, providing evidence that Fe_3O_4 was dispersed throughout the material. According to the results in **Figures 5(a) - 5(b)**, magnetite (Fe_3O_4) is a bright particle that is uniformly distributed inside the paraffin-embedded layer, while some of it is concentrated in the layer facing down the paraffin [44]. In the case of the PCM-A4 sample, it can be seen that the ratio of paraffin to Fe_3O_4 is balanced. This is because the total mass compositions of paraffin and Fe_3O_4 were the same. For PCM with a composition of PCM-A1, the amount of paraffin dominated that of Fe_3O_4. In addition, the EDX analysis shown in **Figures 5(c) - 5(d)** confirmed the distribution of Fe_3O_4 between the paraffin layers and the formation of hybrid nano-Fe_3O_4 based PCM. Hence, shape-stabilized PCM have been developed [45]. This was confirmed by comparing the C, O, and Fe percentages. The EDX results are listed in **Table 4**.

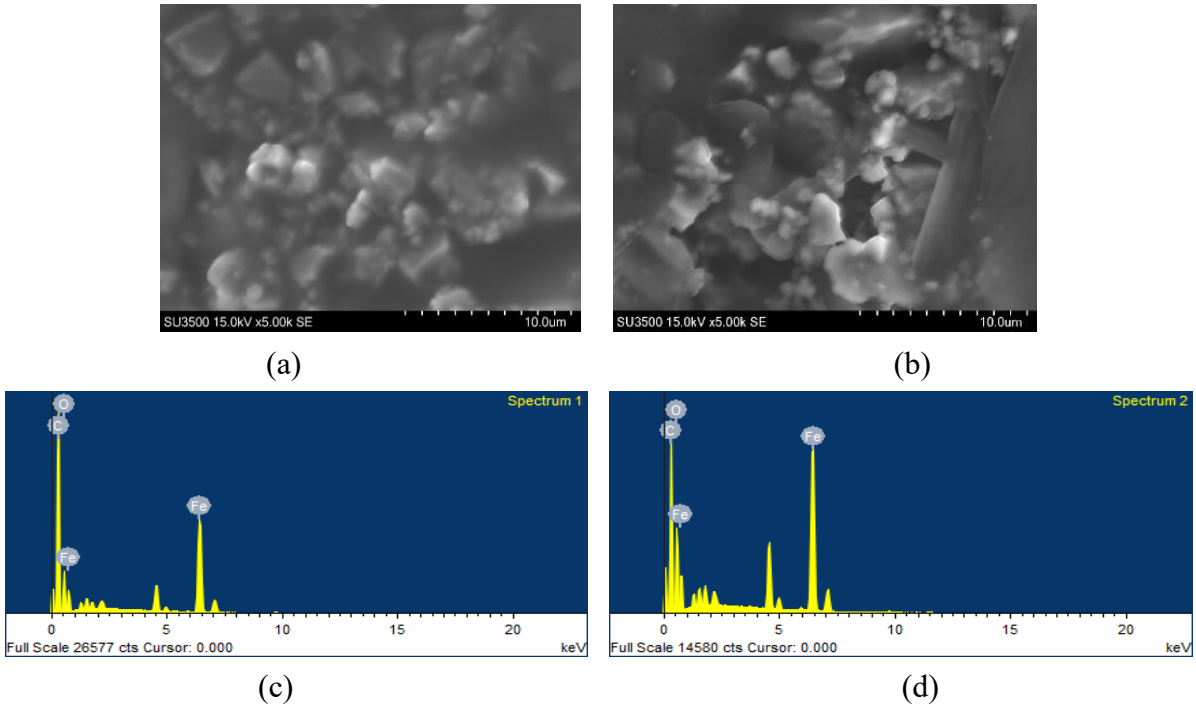

Figure 5 (a) SEM images of PCM-A1, (b) SEM images of PCM-A4, (c) EDX analysis of PCM-A1, and (d) EDX analysis of PCM-A4.

Table 4 EDX Results of the PCM.

Sample	Element	Atomic%
PCM-A1	C	76.71
	O	15.70
	Fe	7.59
	Totals	100
PCM-A4	C	68.98
	O	20.67
	Fe	10.35
	Totals	100

Magnentic analysis of PCM

The shape of the hysteresis curve of a particular material provides significant information regarding its magnetic behavior. The magnetic properties of the PCM measured using VSM250 are presented in **Figure 6**. The magnetization curve illustrates the saturation magnetization (Ms) versus magnetic field (H), confirming the presence of superparamagnetic iron oxide nanoparticles [46,47]. The saturation magnetization, coercivity, and retention values were derived from the hysteresis curves. The magnetic property parameters of the PCM are summarized in **Table 5**. The saturation magnetization (Ms) of the 50 vol% Fe_3O_4 PCM is 30.40 emu/g, which is lower than that reported by Hastak *et al.* who obtained a magnetization of 38.86 emu/g. This discrepancy was attributed to the presence of a non-magnetic paraffin mixture.

Subsequently, the magnetization value decreased by ~10% - 4% based on the amount of Fe_3O_4 added to the composite PCM. The hysteresis curve, resembling the letter S with a very small Hc value, indicates superparamagnetic properties. Another parameter of magnetic properties is the susceptibility value (χ). The susceptibility value quantifies the response of magnetic materials to an external magnetic field. Theoretically,

M = χH; thus, the increase in χ is proportional to the increase in Ms [48]. Further investigation into the increase in Ms with the increase in Fe_3O_4 content in paraffin reveals that it can be related to the value of the magnetic moment and the size of the magnetic domain. Theoretically, the magnetization value is strongly correlated with the magnetic moment and magnetic domain size (Eq. (2)) [48].

$$\mu = \frac{\pi M_x D^3}{6} \quad (2)$$

The results of the VSM analysis on the composite PCM confirmed that the synthesized particles were soft magnetic. The minimal area of the hysteresis curve indicates that the synthesized particles were in close proximity to the superparamagnetic state. These magnetic values were comparable to those reported in previous studies. The addition of magnetite particles to PCM enhances its magnetic properties; however, the composite remains classified as a soft magnetic and superparamagnetic material. This material exhibits a favorable magnetic response and can be readily attracted by magnets [49,50].

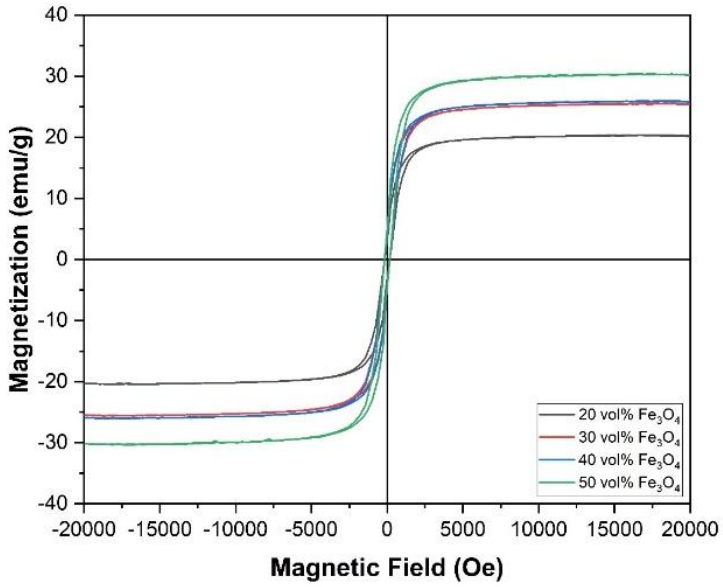

Figure 6 Hysteresis curves of PCM-magnetite.

Table 5 VSM Results of PCM-magnetite composite.

PCM with the addition of Fe_3O_4	Hmax (kOe)	Saturation (emu/g)	Retentivity (emu/g)	Coercivity (Oe)
20% Fe_3O_4	20.233	20.35	3.21	168.67
30% Fe_3O_4	20.233	25.54	3.91	168.73
40% Fe_3O_4	20.214	26.02	4.03	168.66
50% Fe_3O_4	20.241	30.40	4.90	173.27

DSC analyses of PCM

DSC characterizations were performed to analyze the thermal performance of the PCM and their phase-change behavior during the heating and cooling stages. The characterized samples consisted of PCM-A1 and PCM-A4 with sample weights of 5.6 and 5.8 mg, respectively. Characterization was performed according to ASTM D3418-15 test standards and measured using Perkin Elmer DSC 8000 test equipment in an aluminum cell with a nitrogen flow rate of 20 mL/min.

Figures 7(a) - 7(b) are the results of DSC characterization comparison between PCM-A1 and

PCM-A2 samples at 1.5 cycles with an initial temperature of 30 °C and then heated to 100 °C with a temperature increase of 10 °C/min. In the first and fifth steps, PCM melting occurs, whereas in the third step, PCM solidification occurs. The coverage of the heat flow during the heat absorption and heat release process in the PCM-A1 sample, which contained 20 vol% Fe_3O_4 suggested a wider coverage than the PCM-A4 sample with the addition of 50 vol% Fe_3O_4. **Figures 7(a) - 7(b)** confirm that the PCM cycles can be repeated and do not exhibit a shift in the heat flow and thus remain stable [42]. The PCM melting process was found to be endothermic, as illustrated in **Figure 7(c)**. Results indicate that the enthalpy values for the PCM-A4 and PCM-A1 samples were 17.13 and 55.28 J/g, respectively. The addition of Fe_3O_4 led to a decrease in the enthalpy and heat storage capacity of the PCM. However, this resulted in a significant increase in the thermal absorption region. The endothermic peak in the graph corresponds to the melting point of the PCM. In this study, the melting points for the PCM-A1 and PCM-A4 samples were found to be 56.67 and 56.81 °C, respectively.

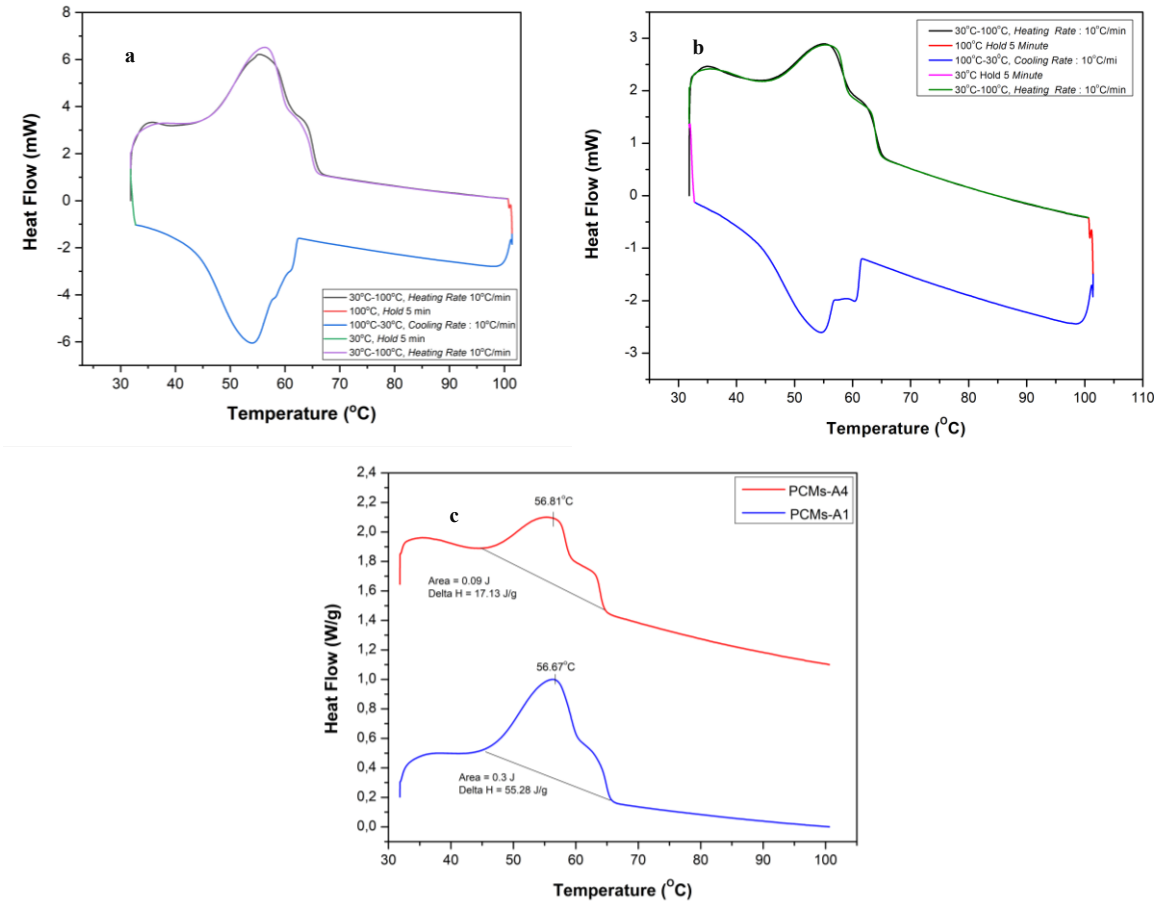

Figure 7 DSC results (a) 1.5 cycles of PCM-A1, (b) 1.5 cycles of PCM-A4, and (c) comparison of endothermic analysis of PCM-A1 and PCM-A4.

Thermal conductivity of PCM

The thermal conductivity of the PCM was investigated to determine their ability to transfer heat from a heat source. In this investigation, the thermal conductivity test of PCM was examined through tests conducted on the PCM-A4 and PCM-A1 samples. The results of the thermal conductivity characterization are shown in **Table 6** and were comparedision with the results of previous research.

Thermal energy can be transmitted through solids in various ways, such as through electrical carriers (electrons or holes), lattice waves (phonons), spin waves, electromagnetic waves, and other excitations [51]. The addition of magnetite particles to paraffin can

improve the thermal conductivity because magnetite contains iron (Fe), which allows thermal energy to flow through Fe electrons instead of the usual vibrations and rotations of the molecular chains in paraffin polymers. Some of the kinetic energy in the free electrons is transferred as vibrational energy to the atoms moving from the hot to cold regions. The magnetite particles in paraffin serve as fillers and act as heat carriers and thermal pathways during the melting and solidification of phase change materials (PCM). As a result, microconvection and thermophoresis can occur more quickly, and the heat transfer in paraffin-magnetite composites can be enhanced [52,53]. Magnetite particles can also boost the endothermic and exothermic reactions of PCM owing to their high thermal conductivities.

Table 6 Thermal conductivity of PCM at ambient temperature.

No	PCM Sample Composition	Thermal Conductivity (W/mK)	Ref
1	PCM-A1	0.37	This work
2	PCM-A4	0.54	This work
3	Paraffin 90 wt % Fe_3O_4 10 wt%	0.37	[26]
4	Paraffin 80 wt % Fe_3O_4 20 wt%	0.40	[26]
5	Pure Paraffin	0.23	[54]
6	Pure magnetite Fe_3O_4	9.7	[51]

The following text provides an analysis of the thermal conductivities of PCM-A4 and PCM-A1, with the results indicating a higher thermal conductivity in PCM-A4 at 0.54 W/m.K compared to PCM-A1 at 0.37 W/mK. This increase in thermal conductivity is attributed to the addition of magnetite (Fe_3O_4) particles, compared to pure paraffin, which has a thermal conductivity of 0.23 W/m·K. Furthermore, the thermal conductivity obtained in this study aligns well with previous research [55]. It is important to note that a higher thermal conductivity in PCM is necessary to enhance the heat transfer from the heat source to the PCM in a shorter period of time, as suggested by previous studies [31,37].

Temperature distribution on concrete

The results obtained from the tests exhibit an exponential curve due to the endothermic process, which rises periodically and is directly proportional to the increase in temperature and time. As the solidification process takes place by gradually lowering the temperature to room temperature at 28 °C, the graph exhibits a decline due to the exothermic event, resulting in an exponential decrease. The temperature distribution results are shown in **Figure 8**. Heat is transferred from the heater, which serves as the heat source, to the concrete and copper tubes via conduction, which can be classified as sensible heat as the temperature changes. Conversely, in PCM, a phase change reaction occurs from solid to liquid (melting) without a change in temperature and can be classified as latent heat. When the heater was turned off during the cooling process, the PCM began to release latent heat, and another phase change transformation occurred (solidification) [13,56].

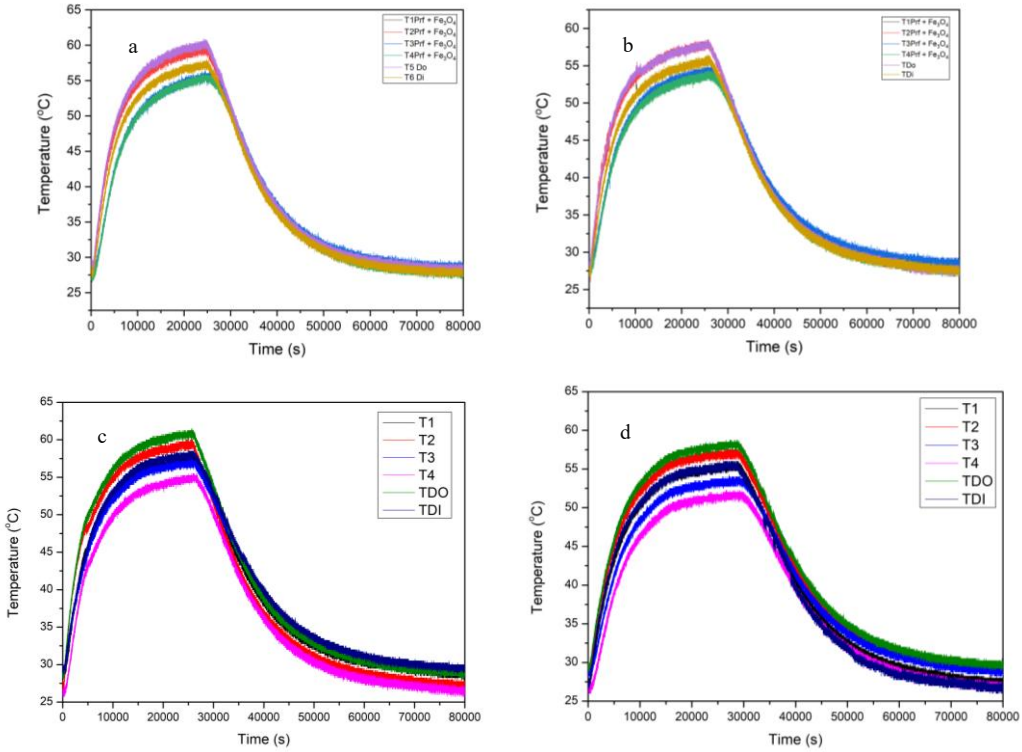

Figure 8 Temperature distribution results (a) PCM-A1, (b) PCM-A2, (c) PCM-A3, (d) and PCM-A4.

In the PCM-A1 and PCM-A3 samples, the thermal absorption was greater than that of the other samples, because the addition of a large amount of paraffin affected the phase changes process [57,58]. The results of the thermal distribution test prove that the PCM-encapsulated concrete can withstand heat and store thermal energy. Furthermore, the maximum stress that the concrete can withstand is reduced as the fraction of PCM increases. The low intensity of PCM reduces the global intensity of concrete. According to the Chinese national standard GB/T 20473-2006 (insulation and mortar in buildings), the maximum tolerable stress of concrete blocks should be higher than 0.4 MPa to meet the demand of a building material. Thus, 15% of PCM was the optimal mass fraction when concrete-based PCM was produced [54,59,60]. **Figure 8** suggests that PCM from the 4 compositions have an average critical temperature value of 56.7 °C with different crisis times. This occurs because of the large amount of magnetite added to PCM, which that affects the longer melting-liquid phase process [61,62]. The longest critical time in the PCM-A4 PCM is 28,951 s.

Conclusions

Paraffin-magnetite (Fe_3O_4) PCM encapsulated in tubes embedded in concrete was prepared and analyzed. XRD characterization showed that Fe_3O_4 and paraffin had cubic and monoclinic crystal phases. The FTIR results showed that magnetite (Fe_3O_4) was successfully distributed on the paraffin filler in the PCM. In addition, magnetite particles were evenly distributed inside the PCM, confirmed by the SEM-EDX morphology results. In contrast, VSM analysis showed that the addition of magnetite increased the saturation magnetization. DSC analysis suggested that the endothermic peak occurred at the highest temperature of 56.81 °C for PCM-A4 and PCM were confirmed to be stable as thermal energy storage. The highest thermal conductivity was obtained for PCM-A4 composition of 0.54 W/m·K. Additionally, the results of the thermal distribution analysis confirmed that the PCM could store and transmit heat. Moreover, the paraffin-magnetite composites studied in this investigation have potential applications in thermal energy storage owing to the thermal properties of the composites. These results demonstrate that the composite has potential as a thermal energy storage medium in building materials. However, this study has

certain limitations that warrant further investigation. The long-term thermal stability and cycling reliability of the composite remain underexplored, particularly in relation to repeated phase transitions and environmental exposure. To address potential agglomeration and improve dispersion uniformity, future studies should consider surface tension modification strategies, such as the incorporation of surfactants. Additionally, while this research focused on Fe_3O_4 due to its natural abundance and magnetic responsiveness, alternative filler materials - such as metal oxides and carbon-based nanomaterials - may offer improved thermal performance. Future research should investigate these advanced materials and evaluate their structural integrity, scalability, and integration potential in real-world building thermal management systems.

Acknowledgements

The authors would like to thank the Research Center for Advanced Materials, National Research and Innovation Agency (BRIN), Indonesia for the facilities used in this research. The authors also acknowledge the PMDSU (Master to Doctoral Education) Batch VIII scholarship program from the Ministry of Education, Culture, Research and Technology of Indonesia for financial support, and the Postgraduate Physics Program at Universitas Sumatera Utara, Indonesia for their support and encouragement.

Declaration of Generative AI in Scientific Writing

The authors acknowledge the use of ChatGPT (OpenAI) in the preparation of this manuscript, specifically for language editing and grammar correction. No content generation, scientific idea creation, or data interpretation was performed by AI. The authors take full responsibility for the content and conclusions of this work.

Credit author statement

Widya Sonita Gultom: Writing - original draft; Investigation; Formal analysis; Project administration. **Timbangen Sembiring**: Writing - review & editing; Validation; Supervision; Conceptualization; Funding acquisition. **Anggito Pringgo Tetuko**: Validation; Supervision; Conceptualization; Resources; **Muhammad Fauzi**: Methodology; Data curation; Investigation. **Amdy Fachredzy**: Project administration. **Eko Arief Setiadi**: Validation. **Nining Sumawati Asri**: Validation. **Ayu Yuswita Sari**: Validation. **Martha Rianna**: Validation. **Erna Frida**: Validation. **Achmad Maulana Soehada Sebayang:** Validation.

References

[1] MA Abdel-Mawla, MA Hassan and A Khalil. Phase change materials in thermally activated building systems: A comprehensive review. *International Journal of Energy Research* 2022; **46(9)**, 11676-11717.

[2] PKS Rathore, NK Gupta, D Yadav, SK Shukla and S Kaul. Thermal performance of the building envelope integrated with phase change material for thermal energy storage: An updated review. *Sustainable Cities and Society* 2022; **79**, 103690.

[3] Q Al-Yasiri and M Szabó. Thermal performance of concrete bricks based phase change material encapsulated by various aluminium containers: An experimental study under Iraqi hot climate conditions. *Journal of Energy Storage* 2021; **40**, 102710.

[4] S Rostami, M Afrand, A Shahsavar, M Sheikholeslami, R Kalbasi, S Aghakhani, MS Shadloo and HF Oztop. A review of melting and freezing processes of PCM/nano-PCM and their application in energy storage. *Energy* 2020; **211**, 118698.

[5] FR Saeed, EC Serban, E Vasile, M Al-Timimi, WHA Al-Banda, MZA Abdullah, I Stamatin, A Cucu, SM Iordache, S Voinea and AE Balan. Nanomagnetite enhanced paraffin for thermal energy storage applications. *Digest Journal of Nanomaterials and Biostructures* 2017; **12(2)**, 273-280.

[6] E Alehosseini and SM Jafari. Nanoencapsulation of phase change materials (PCM) and their applications in various fields for energy storage and management. *Advances in Colloid and Interface Science* 2020; **283**, 102226.

[7] S Koohi-Fayegh and MA Rosen. A review of energy storage types, applications and recent developments. *Journal of Energy Storage* 2020; **27**, 101047.

[8] M Usman, F Siddiqui, A Ehsan, RA Sadaqat and A Hussain. Improvement of thermal conductivity

of paraffin wax, a phase change material with graphite powder. *In*: Proceedings of the 17th International Bhurban Conference on Applied Sciences and Technology (IBCAST), Islamabad, Pakistan. 2020, p. 16-25.

[9] S Wu, T Yan, Z Kuai and W Pan. Thermal conductivity enhancement on phase change materials for thermal energy storage: A review. *Renewable and Sustainable Energy Reviews* 2020; **25**, 251-295.

[10] M Amin, F Afriyanti and N Putra. Thermal properties of paraffin based nano-phase change material as thermal energy storage. *IOP Conference Series: Earth and Environmental Science* 2018; **105**, 012028.

[11] T Zhao, M Zheng, A Munis, J Hu, H Teng and L Wei. Corrosion behaviours of typical metals in molten hydrate salt of $Na_2HPO_4 \cdot 12H_2O$ - $Na_2SO_4 \cdot 10H_2O$ for thermal energy storage. *Corrosion Engineering, Science and Technology* 2019; **54(5)**, 379-388.

[12] B Lu, Y Zhang, J Zhang, J Zhu, H Zhao and Z Wang. Preparation, optimization and thermal characterization of paraffin/nano-Fe3O4 composite phase change material for solar thermal energy storage. *Journal of Energy Storage* 2022; **46**, 103928.

[13] AP Tetuko, AMS Sebayang, A Fachredzy, EA Setiadi, NS Asri, AY Sari, F Purnomo, C Muslih, MA Fajrin and P Sebayang. Encapsulation of paraffin-magnetite, paraffin, and polyethylene glycol in concretes as thermal energy storage. *Journal of Energy Storage* 2023; **68**, 107684.

[14] C Liu, L Wang, Y Li, X Diao, C Dong, A Li and X Chen. Fe_3O_4/carbon-decorated graphene boosts photothermal conversion and storage of phase change materials. *Journal of Colloid and Interface Science* 2024; **657**, 590-597.

[15] IA Laghari, M Samykano, AK Pandey, Z Said, K Kadirgma and VV Tyagi. Thermal conductivity and thermal properties enhancement of paraffin/ titanium oxide based nano enhanced phase change materials for energy storage. *In*: Proceedings of the Advances in Science and Engineering Technology International Conferences (ASET), Dubai, United Arab Emirates. 2022.

[16] R Bharathiraja, T Ramkumar and M Selvakumar. Studies on the thermal characteristics of nano-enhanced paraffin wax phase change material (PCM) for thermal storage applications. *Journal of Energy Storage* 2023; **73**, 109216.

[17] SK Singh, SK Verma and R Kumar. Thermal performance and behavior analysis of SiO2, Al_2O_3 and MgO based nano-enhanced phase-changing materials, latent heat thermal energy storage system. *Journal of Energy Storage* 2022; **48**, 103977.

[18] MA Fikri, AK Pandey, M Samykano, K Kadirgama, M George, R Saidur, J Selvaraj, NA Rahim, K Sharma and VV Tyagi. Thermal conductivity, reliability, and stability assessment of phase change material (PCM) doped with functionalized multi-wall carbon nanotubes (FMWCNTs). *Journal of Energy Storage* 2022; **50**, 104676.

[19] C Liu, L Wang, Y Li, X Diao, C Dong, A Li and X Chen. Fe_3O_4/carbon-decorated graphene boosts photothermal conversion and storage of phase change materials. *Journal of Colloid and Interface Science* 2024; **657**, 590-597.

[20] P Zhang, Y Qiu, C Ye and Q Li. Anisotropically conductive phase change composites enabled by aligned continuous carbon fibers for full-spectrum solar thermal energy harvesting. *Chemical Engineering Journal* 2023; **461**, 141940.

[21] SS Prabhu, P Selvakumar and JS Heric. Thermal stability and behaviour of paraffin nano Al_2O_3, graphene and surfactant sodium oleate composite as phase change material. *Materials Research Express* 2022; **9(11)**, 115504.

[22] W He, Y Zhuang, Y Chen and C Wang. Thermo-magnetic convection regulating the solidification behavior and energy storage of Fe_3O_4 nanoparticles composited paraffin wax under the magnetic-field. *Applied Thermal Engineering* 2022; **214**, 118617.

[23] W He, Y Zhuang, Y Chen and C Wang. Experimental and numerical investigations on the melting behavior of Fe3O4 nanoparticles composited paraffin wax in a cubic cavity under a magnetic-field. *International Journal of Thermal Sciences* 2023; **184**, 107961.

[24] D Hu, L Han, W Zhou, P Li, Y Huang, Z Yang and X Jia. Flexible phase change composite based on loading paraffin into cross-linked CNT/SBS network for thermal management and thermal storage. *Chemical Engineering Journal* 2022; **437**, 135056.

[25] SW Sharshir, NM El-Shafai, MM Ibrahim, AW Kandeal, HS El-Sheshtawy and MS Ramadan. Effect of copper oxide/cobalt oxide nanocomposite on phase change material for direct/indirect solar energy applications: Experimental investigation. *Journal of Energy Storage* 2021; **38**, 102526.

[26] N Şahan, M Fois and H Paksoy. Improving thermal conductivity phase change materials - A study of paraffin nanomagnetite composites. *Solar Energy Materials and Solar Cells* 2015; **137**, 61-67.

[27] N Sahan and HO Paksoy. Thermal enhancement of paraffin as a phase change material with nanomagnetite. *Solar Energy Materials and Solar Cells* 2014; **126**, 56-61.

[28] S Afgan, RA Khushnood, SA Memon and N Iqbal. Development of structural thermal energy storage concrete using paraffin intruded lightweight aggregate with nano-refined modified encapsulation paste layer. *Construction and Building Materials* 2019; **228**, 116768.

[29] P Sukontasukkul, P Uthaichotirat, T Sangpet, K Sisomphon, M Newlands, A Siripanichgorn and P Chindaprasirt. Thermal properties of lightweight concrete incorporating high contents of phase change materials. *Construction and Building Materials* 2019; **207**, 431-439.

[30] Q Al-Yasiri and M Szabo. Effect of encapsulation area on the thermal performance of PCM incorporated concrete bricks: A case study under Iraq summer conditions. *Case Studies in Construction Materials* 2021; **15**, e00686.

[31] MM Alsaadawi, M Amin and AM Tahwia. Thermal, mechanical and microstructural properties of sustainable concrete incorporating Phase change materials. *Construction and Building Materials* 2022; **356**, 129300.

[32] H Ying, S Wang, Z Lu, B Liu, L Cui, X Quan, K Liu and N Zhao. Development and thermal response of concrete incorporated with multi-stage phase change materials-aggregates for application in seasonally frozen regions. *Journal of Building Engineering* 2023; **71**, 106562.

[33] M Zandie, A Moghaddas, A Kazemi, M Ahmadi, HN Feshkache, MH Ahmadi and M Sharifpur. The impact of employing a magnetic field as well as Fe_3O_4 nanoparticles on the performance of phase change materials. *Engineering Applications of Computational Fluid Mechanics* 2022; **16(1)**, 196-214.

[34] P Sukontasukkul, P Uthaichotirat, T Sangpet, K Sisomphon, M Newlands, A Siripanichgorn and P Chindaprasirt. Thermal properties of lightweight concrete incorporating high contents of phase change materials. *Construction and Building Materials* 2019; **207**, 431-439.

[35] S Ilyas, B Abdullah and D Tahir. X-ray diffraction analysis of nanocomposite Fe_3O_4/activated carbon by Williamson–Hall and size-strain plot methods. *Nano-Structures and Nano-Objects* 2019; **20**, 100396.

[36] HH Elnahas, SM Abdou, H El-Zahed and A Abdeldaym. Structural, morphological and mechanical properties of gamma irradiated low density polyethylene/paraffin wax blends. *Radiation Physics and Chemistry* 2018; **151**, 217-224.

[37] S Wu, Y Zhou, W Gao, Z Zhang, A Liu, R Cai, C Wu, X Peng, S Li, C Li, W Yu and Z Huang. Preparation and properties of shape-stable phase change material with enhanced thermal conductivity based on SiC porous ceramic carrier made of iron tailings. *Applied Energy* 2014; **355**, 122256.

[38] M Rianna, EA Setiadi, S Susiani, AMS Sebayang, M Fauzi, MK Hussain, K Yuliana, NS Asri, LF Nurdiyansah, AP Tetuko and P Sebayang. Enhanced calcination temperatures of $SrFe_{12}O_{19}$ synthesized by local iron sand from Lombok Island. *Case Studies in Chemical and Environmental Engineering* 2023; **8**, 100530.

[39] DA Sahbaz, A Yakar and U Gündüz. Magnetic Fe_3O_4 -chitosan micro- and nanoparticles for wastewater treatment. *Particulate Science and Technology* 2019; **37**, 732-740.

[40] Y Li, J Yu, Z Cao, W Du, Y Zhang and Y Zou. Preparation and characterization of nano-

Fe_3O_4/paraffin encapsulated isocyanate microcapsule by electromagnetic controlled rupture for self-healing cementitious materials. *Construction and Building Materials* 2020; **265**, 120703.

[41] MS Mert, HH Mert and CY Gumus. Preparation and characterization of paraffin microcapsules for energy-saving applications. *Journal of Applied Polymer Science* 2019; **136(33)**, 47874.

[42] D Hu, L Han, W Zhou, P Li, Y Huang, Z Yang and X Jia. Flexible phase change composite based on loading paraffin into cross-linked CNT/SBS network for thermal management and thermal storage. *Chemical Engineering Journal* 2022; **437**, 135056.

[43] S Park, Y Lee, YS Kim, HM Lee, JH Kim, IW Cheong and WG Koh. Magnetic nanoparticle-embedded PCM nanocapsules based on paraffin core and polyurea shell. *Colloids and Surfaces A: Physicochemical and Engineering Aspects* 2014; **450**, 46-51

[44] SW Sharshir, NM El-Shafai, MM Ibrahim, AW Kandeal, HS El-Sheshtawy, MS Ramadan, M Rashad and IM El-Mehasseb. Effect of copper oxide/cobalt oxide nanocomposite on phase change material for direct/indirect solar energy applications: Experimental investigation. *Journal of Energy Storage* 2021; **38**, 102526.

[45] Y Zhang, S Zheng, S Zhu, J Ma, Z Sun and M Farid. Evaluation of paraffin infiltrated in various porous silica matrices as shape-stabilized phase change materials for thermal energy storage. *Energy Conversion and Management* 2018; **171**, 361-370.

[46] MA Javid, T Habib and K Nadeem. Rheological properties of synthesized Fe_3O_4 in non-newtonian fluids. *Materials Today: Proceedings* 2021; **47**, S125-S133.

[47] PM Kumar, D Sudarvizhi, PMJ Stalin, A Aarif, R Abhinandhana, A Renuprasanth, V Sathya and NT Ezhilan. Thermal characteristics analysis of a phase change material under the influence of nanoparticles. *Materials Today: Proceedings* 2021; **45**, 7876-7880.

[48] W He, Y Zhuang, Y Chen and C Wang. Thermo-magnetic convection regulating the solidification behavior and energy storage of Fe_3O_4 nanoparticles composited paraffin wax under the magnetic-field. *Applied Thermal Engineering* 2022; **214**, 118617.

[49] G Antarnusa and E Suharyadi. A synthesis of polyethylene glycol (PEG)-coated magnetite Fe_3O_4 nanoparticles and their characteristics for enhancement of biosensor. *Materials Research Express* 2020; **7(5)**, 056103.

[50] DD Dixit and A Pattamatta. Effect of uniform external magnetic-field on natural convection heat transfer in a cubical cavity filled with magnetic nano-dispersion. *International Journal of Heat and Mass Transfer* 2020; **146**, 118828.

[51] M Zandie, A Moghaddas, A Kazemi, M Ahmadi, HN Feshkache, MH Ahmadi and M Sharifpur. The impact of employing a magnetic field as well as Fe_3O_4 nanoparticles on the performance of phase change materials. *Engineering Applications of Computational Fluid Mechanics* 2022; **16(1)**, 196-214.

[52] T Wangler, N Roussel, FP Bos, TAM Salet and RJ Flatt. Digital concrete: A review. *Cement and Concrete Research* 2019; **123**, 105780.

[53] IB Rahardja, VNC Surbakti and AL Siregar. Empowering abu cangkang kelapa sawit terhadap kualitas bata beton ringan (light-weight concrete) (*in Indonesian*). *Jurnal Teknologi* 2022; **14(1)**, 119-126.

[54] Z Zhang, Y Liu, J Wang, L Sun, T Xie, K Yang and Z Li. Preparation and characterization of high efficiency microencapsulated phase change material based on paraffin wax core and SiO_2 shell derived from sodium silicate precursor. *Colloids and Surfaces A: Physicochemical and Engineering Aspects* 2021; **625**, 126905.

[55] AP Tetuko, AMS Sebayang, A Fachredzy, EA Setiadi, NS Asri, AY Sari, F Purnomo, C Muslih, MA Fajrin and Sebayang. Encapsulation of paraffin-magnetite, paraffin, and polyethylene glycol in concretes as thermal energy storage. *Journal of Energy Storage* 2023; **68**, 107684.

[56] AP Tetuko, LF Nurdiyansah, M Addin, EA Setiadi, M Ginting and P Sebayang. Magnetic nanofluids as heat transfer media in heat pipes. *Advances in Natural Sciences: Nanoscience and Nanotechnology* 2020; **11(2)**, 025002.

[57] P Das and P Tiwari. Thermal degradation study of waste polyethylene terephthalate (PET) under inert and oxidative environments. *Thermochim Acta* 2019; **679**, 178340.

[58] S Wu, T Yan, Z Kuai and W Pa. Thermal conductivity enhancement on phase change materials for thermal energy storage: A review. *Energy Storage Materials* 2020; **25**, 251-295.

[59] Y Yang, W Wu, S Fu and H Zhang. Study of a novel ceramsite-based shape-stabilized composite phase change material (PCM) for energy conservation in buildings. *Construction and Building Materials* 2020; **246**, 118479.

[60] SS Paneliya, S Khanna, AP Singh, YK Patel, A Vanpariya, NH Makani, R Banerjee and I Mukhopadhyay. Core shell paraffin/silica nanocomposite: A promising phase change material for thermal energy storage. *Renewable Energy* 2021; **167**, 591-599.

[61] YM Baek, PS Shin, JH Kim, HS Park, KL DeVries and JM Park. Thermal transfer, interfacial, and mechanical properties of carbon fiber/polycarbonate-CNT composites using infrared thermography. *Polymer Testing* 2020; **81**, 106247.

[62] H Jouhara, A Żabnieńska-Góra, N Khordehgah, D Ahmad and T Lipinski. Latent thermal energy storage technologies and applications: A review. *International Journal of Thermofluids* 2020; **5**, 100039.